Limit Amplitude of Galloping Bluff Cylinders

L. E. Ericsson*
Lockheed Missiles & Space Company, Inc., Sunnyvale, California

An analysis is presented for the galloping in a single degree of freedom of bluff cross sections. The limit cycle oscillation phenomenon is studied in particular, and the maximum possible galloping amplitude of an arbitrary cross section is derived. The theoretical results are found to be in good agreement with available experimental results.

Nomenclature

b = span
c = two-dimensional chord length
$c_{n\alpha}$ = $\partial c_n/\partial\alpha$
c_{n_z} = $\partial c_n/\partial(\dot{z}/V)$
$c_{\bar{n}_{\dot{z}}}$ = integrated mean value
C_p = pressure, coefficient, $(p-p_\infty)/(\rho V^2/2)$
d' = sectional drag, coefficient $c_d = d'/(\rho V^2/2)c$
f = frequency
h = maximum cross-sectional height
l = sectonal lift, coefficient $c_l = 1/(\rho V^2/2)c$
n = sectional normal force, coefficient $c_n = n/(\rho V^2/2)c$
r = corner radius
Re, Re_x = Reynolds number, $Re = Vc/\nu$, $Re_x = Vx/\nu$
t = time
u'/U = tubulence intensity
V = cross-flow velocity
$\bar{V}$ = reduced velocity, $\bar{V} = V/fh$
z = vertical coordinate
$\dot{z}$ = $\partial z/\partial t$
α = angle of attack
Δz = oscillation amplitude
δ = boundary-layer thickness
ω = angular oscillation frequency, $\omega = 2\pi f$

Subscripts

lim = limit
max = maximum
min = minimum
s = separated flow
0 = initial value
$1,2,3$ = numbering subscripts

Superscript

i = separation-induced, e.g., $\Delta^i c_n$ = separation-induced normal force

Introduction

THE galloping vibration is a well-known problem.[1] However, the galloping response is still difficult to predict as the relevant experimental data must first be obtained.[2] The purpose of the present paper is not to review past progress but rather to add new information gathered in the process of analyzing the problem of galloping cable trays encounterd on the Space Shuttle launch vehicle.[3,4] As the source of the galloping is the adverse fluid dynamics generated by separated flow, experimental results have to be used in the analysis, bringing up the age-old problem of Reynolds number scaling. In the case of the Space Shuttle analysis[3,4] the cable trays were embedded in a thick viscous shear layer, complicating the scaling problem. The applied solution was to develop means to obtain the limiting, most adverse loads and use them in the analysis. Since galloping cables often are submerged in the ground wind shear layer a similar limiting analysis is needed to define the most adverse conditions possible and the associated maximum possible galloping amplitudes. Such an analysis is presented in this paper.

Discussion

The effects of separated flow on the normal force characteristics of a drop-shaped low-drag cross section were discussed in Ref. 5, and it was shown how these characteristics cause divergent bending oscillations of a submarine antenna mast. The separation-induced effects on a rectangular cross section are very similar. Both cross sections will experience divergent oscillations in plunge until the limit cycling phenomenon occurs, usually at very large amplitudes.[6] In contrast to what was the case for the small amplitude oscillations of the Space Shuttle cable tray,[3,4] structural damping plays an insignificant role for the large amplitude galloping case to be discussed here. The frequency of the galloping vibration is assumed to be below that for lock-on of Karman vortex shedding.[1,2,7]

A systematic investigation of the static characteristics of rectangular and other noncircular cross sections[8] shows that large negative lift slopes exist at the subscritical Reynolds number $Re = 0.3 \times 10^6$ (Fig. 1). At Reynolds number $Re = 10^6$ large positive lift slopes are generated, except in the case of the small corner radius where supercritical conditions apparently never were established. The importance of the shoulder radius was illustrated by Polhamus[8] (Fig. 2). The figure shows that for $r/c = 0.08$ the "supercritical" $Re = 10^6$ never caused supercritical flow conditions.

Figure 2 demonstrates that the combined large effects of Reynolds number and corner radius can be represented by the Reynolds number based on the corner radius. That this cannot be the whole story, however, is demonstrated by the results[9] in Fig. 3 for a sharp-cornered $c/h = 2$ rectangle. Turbulence levels of up to 8% are reached in a thick smooth-wall boundary layer.[10] The results in Figs. 2 and 3 demonstrate the need for an analysis that can compute the response for the limiting, most adverse characteristics.

Analysis

The supercritical results in Figs. 1 and 2 show that $c_{n\alpha} = c_{l\alpha} + c_d$ is close to thin plate value $c_{n\alpha} = 2\pi$. Apparently, the increased drag makes up for the $c_{l\alpha}$-loss in composing $c_{n\alpha} \approx c_{l\alpha} + c_d$. Subcritical flow results for sharp-cornered rectangular cross sections[11] show that no negative lift is generated for $c/h = 0.5$, in agreement with the findings[11] that self-excited galloping oscillations do not occur for $c/h = 0.5$ (Fig. 4).

The results in Fig. 1 can be represented as is shown in Fig. 5. Two characteristics stand out: 1) the supercritical $c_{n\alpha}$ value

Received March 15, 1983; revision received June 14, 1983.

*Senior Consulting Engineer. Fellow AIAA.

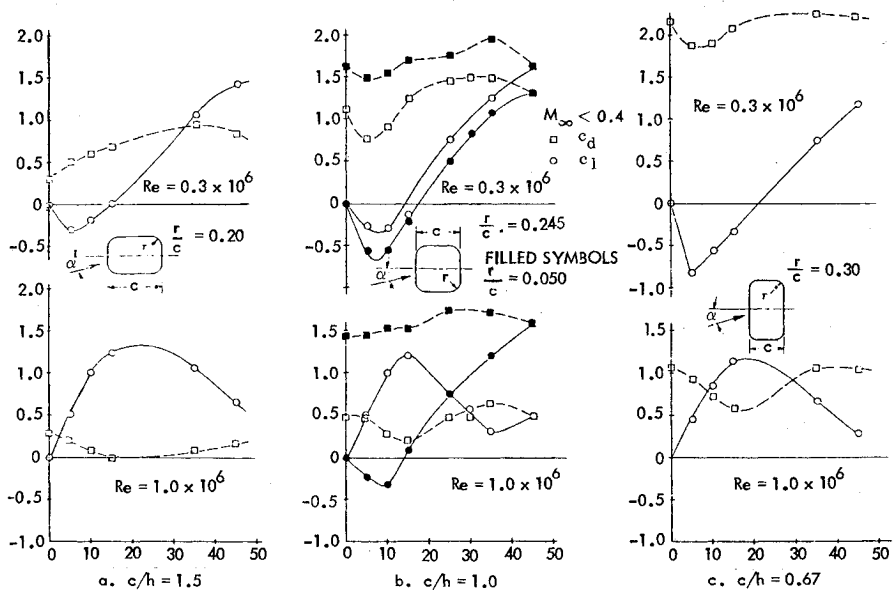

Fig. 1 Aerodynamic characteristics of rectangular cross sections.[8]

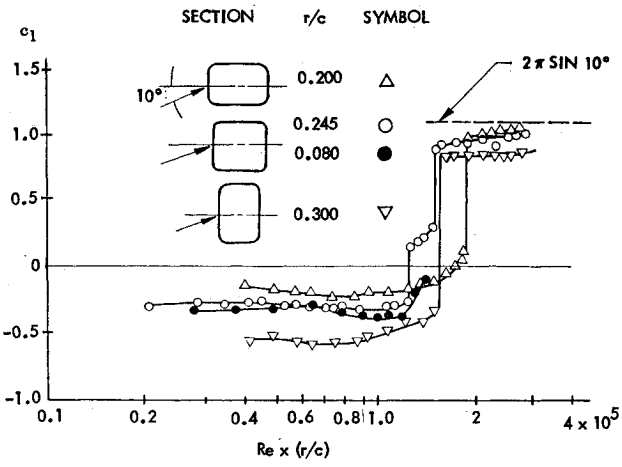

Fig. 2 Combined effect of corner radius and Reynolds number.[8]

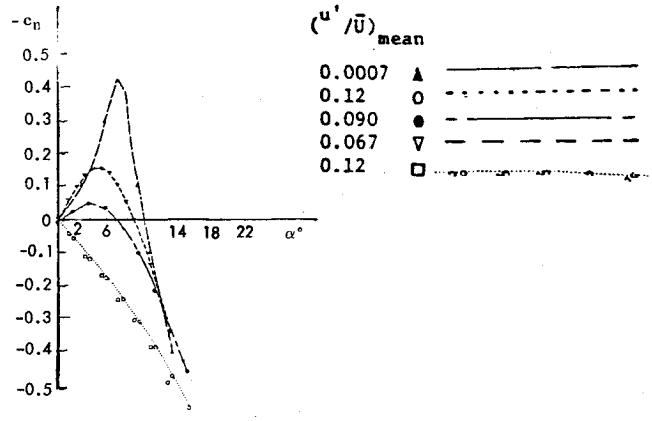

Fig. 3 Effect of freestream turbulence on the normal force characteristics of a $c/h = 2$ rectangular cross section.[9]

is reaching the thin plate value even for $h/c > 1$, and 2) when referenced to the frontal area (the profile height per unit span) the subcritical negative $c_{n\alpha}$ is of attached flow magnitude, i.e.,

$$c_{n\alpha} \approx -2\pi h/c \tag{1}$$

The experimental results reported by Parkinson[11] showed a nonlinear development of the negative normal force before reaching $c_{n_{\min}}$ at $\alpha = \alpha_2$, contrary to the linear behavior measured by Polhamus (Fig. 1) and others[12] on rectangular cross sections. Representing the mean slope for $0 < \alpha < \alpha_2$ by $c_{n\alpha} = c_{n_{\min}}/\alpha_2$ one finds that Parkinson's results[11] are bounded by Eq. (1). It is obvious that, as the mechanical damping is negligible, plunging oscillations will be undamped (divergent) for $\dot{z}/V < \alpha_2$. Not until the angular oscillation amplitude is substantially larger than α_2 will the oscillations become damped. A nonlinear analysis is required for this large amplitude oscillation.

Nonlinear Analysis

In the nonlinear damping analysis performed in Ref. 6 the three possible variations of negative normal force development illustrated in Fig. 6 were investigated. The computed effective damping derivative (the linear measure of the energy dissipation per oscillation cycle) $c_{n\dot{z}}$ for $c/h = 2$ is shown in Fig. 7, where the different curve designations correspond to those for the nonlinear $c_n(\alpha)$ characteristics in Fig. 6. As expected, the linear negative $c_n(\alpha)$ characteristics (dash-dot line) give the most adverse damping characteristics. However, it can be seen that the value $|\dot{z}|/V$ for $c_{n\dot{z}} = 0$, which is the plunging limit cycle amplitude for negligible mechanical damping, is not very sensitive to the detailed damping characteristics at $0 < |\dot{z}|/V < \alpha_2$, a result in basic agreement with past experience for axisymmetric blunt-nosed bodies, limit cycling in pitch.[13]

Limiting Analysis

The experimental results in Figs. 1-3 illustrate the problem of scaling experimental results to apply in the full-scale analysis. The effects of Reynolds number, corner roundness, surface roughness and freestream turbulence present a problem very similar to that encountered in regard to the vortex-induced asymmetric loads generated on a slender body at high angles of attack.[14,15] The solution in the case of the asymmetric vortices was to develop means by which the limiting, largest possible induced side forces could be computed.[16] The same approach will be used here. That is, analytic means will be formulated by which the most adverse cross-sectional characteristics and associated plunging oscillations can be computed.

The key to the limiting analysis is to find the most conservative values (largest magnitudes) of $c_{n_{\min}}$ and α_2 in Fig. 6,

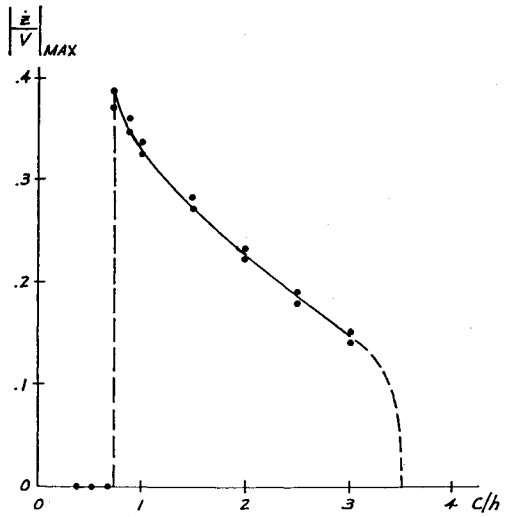

Fig. 4 Galloping cable data for rectangular cross sections.[11]

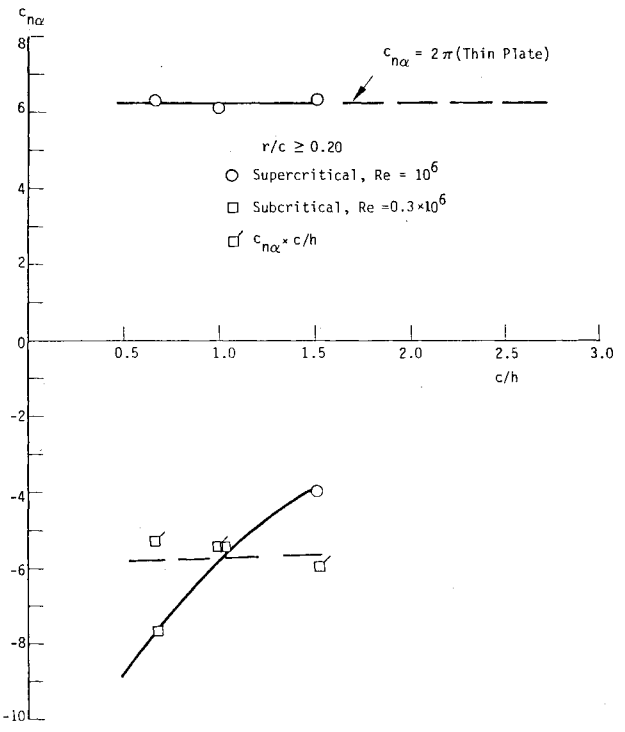

Fig. 5 Normal force slope as a function of rectangular chord-to-height ratio.[3]

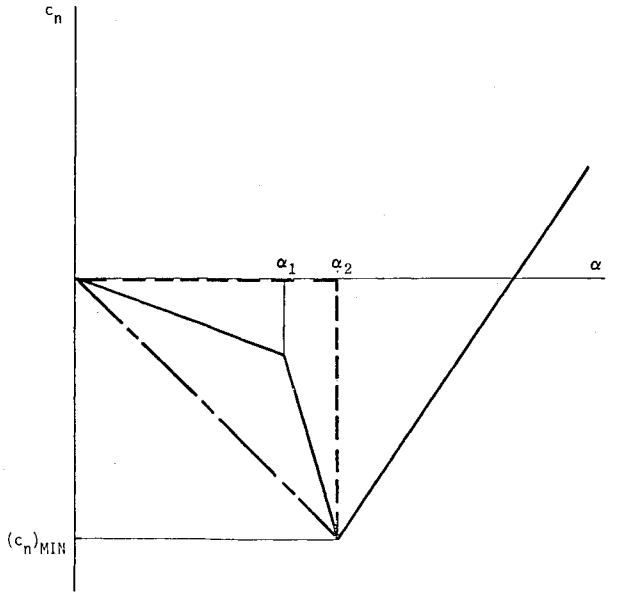

Fig. 6 Nonlinear normal force characteristics.

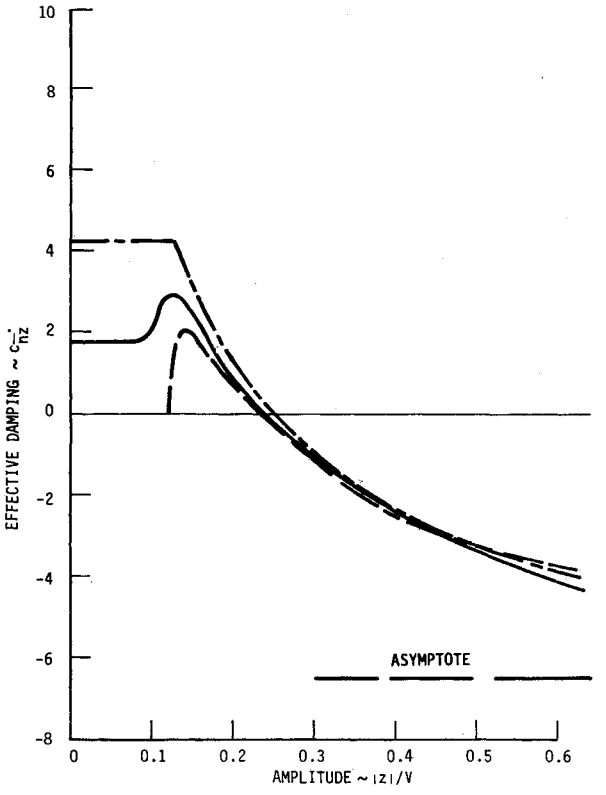

Fig. 7 Effective damping as a function of amplitude for a $c/h=2$ rectangular cross section.[6]

such that they will bound the results for an arbitrary cross section describing either pure plunging oscillations or a combination of plunging and pitching oscillations, as in the case of ice-covered cables[17] (note that $c_{n\alpha}=2\pi$ for $\alpha>\alpha_2$, as was discussed earlier in connection with Fig. 5).

The measured pressures on the square ($c/h=1$) cross section[11] (Fig. 8) show that $c_{n_{\min}}$ is generated by the leeward side (compare $\alpha=0$ with $\alpha=14$ deg). Apparently, the separation bubble closes enough at $\alpha=0$ to generate suction pressures similar to those on a good airfoil. At $\alpha=14$ deg the leeside flow is completely separated, similar to what occurs for a flat plate at high angles of attack. Consequently, the difference between $c_{l_{\max}}$ for a good airfoil (NACA-0012) and c_l for a flat plate at the same angle of attack would represent the maximum magnitue of $c_{n_{\min}}$. The results[18] in Fig. 9 give $c_{n_{\min}}=-0.80$ when extrapolating $c_{l_{\max}}$ for NACA-0012 to $Re\to\infty$. One can see that this value bounds the $c_{n_{\min}}$ results in Figs. 1 and 3. In addition to $c_{n_{\min}}$ one also needs a limiting value for α_2. It signifies when the flow starts reattaching on the windward side (see Fig. 8). This in turn causes the leeward flow to join with the base wake, and the leeside pressures take on the base pressure level (Fig. 8). In the case of a sharp leading edge, the thin airfoil stall occurs when the long bubble no longer reattaches before the trailing edge. The windward side flow process on the rectangular airfoil is this process in the reverse. If the bubbles were similar, which they are not due to the different leading-edge geometries, α_2 would simply be the stall angle for the thin airfoil. The largest value α_2 can

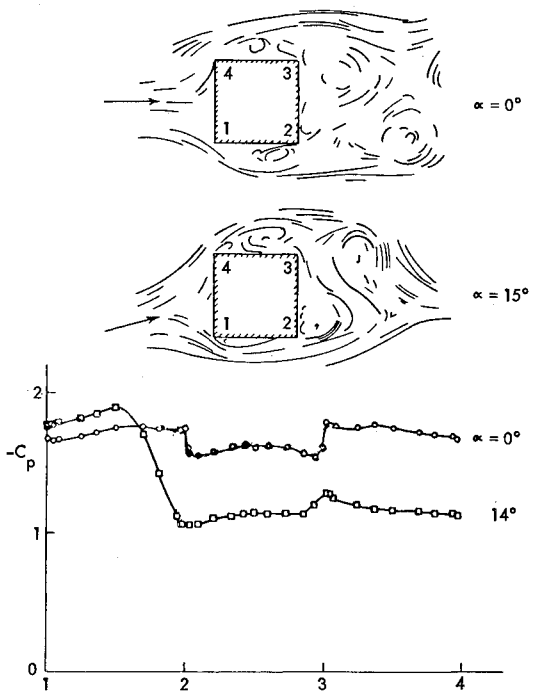

Fig. 8 Flow patterns and surface pressure distribution on a $c/h=1$ cross section.[11]

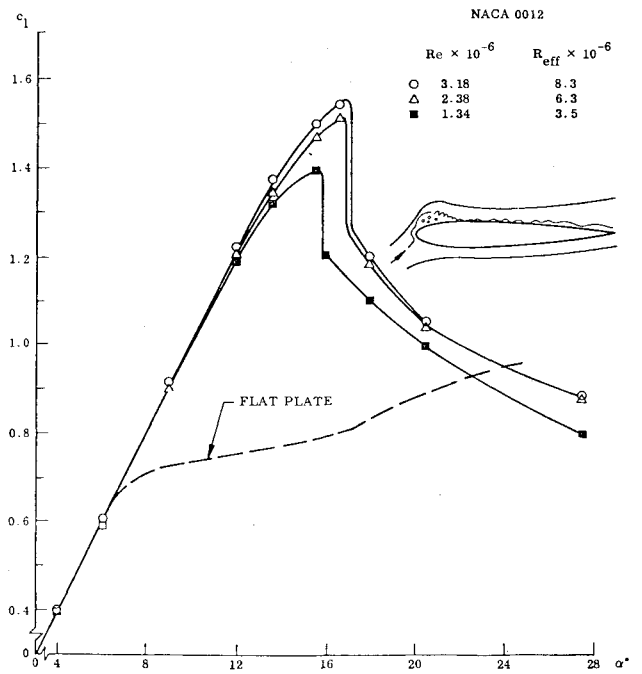

Fig. 9 Lift characteristics for NACA-0012 and a flat plate airfoil.[18]

take is represented by the stall angle for a good airfoil, such as NACA-0012. Figure 9 gives $\alpha_2 < 18$ deg. Again, looking at the results in Figs. 1 and 3, one finds that $\alpha_2 = 18$ deg bounds the experimental values.

With $c_{n_{min}} = -0.80$, $\alpha_2 = 18$ deg $= 0.314$, and $c_n\alpha_3 = 2\pi$ the analysis in Ref. 6 gives the results shown in Fig. 10. For zero mechanical damping $(c_{n\dot{z}})_{min} = 0$ in Fig. 10 gives the following maximum possible limit cycle amplitude for plunging oscillations.

$$(|\dot{z}|/V)_{lim} < 0.55 \qquad (2)$$

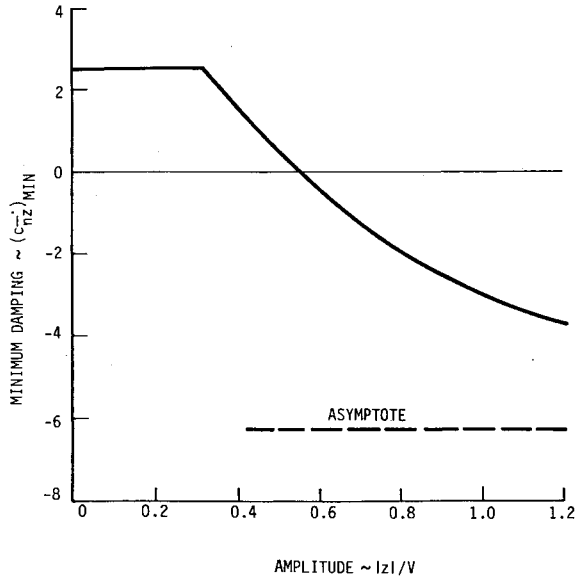

Fig. 10 Minimum effective damping.

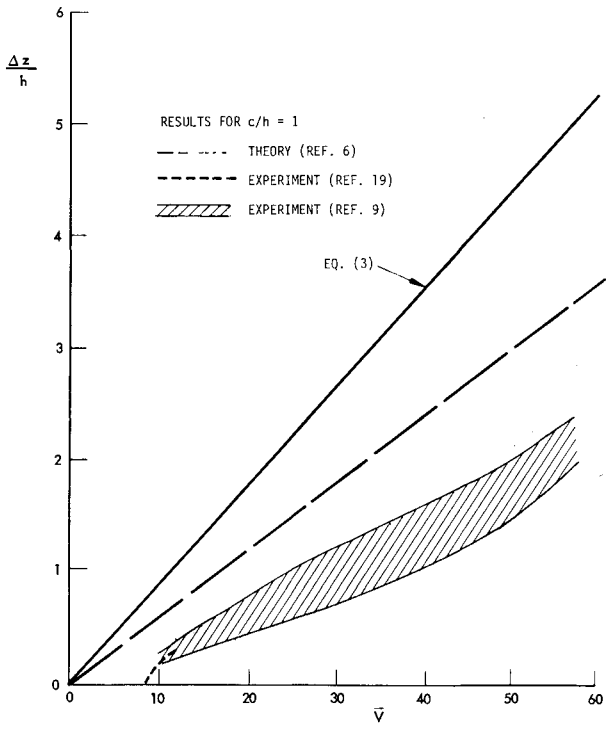

Fig. 11 Limit cycle amplitude as a function of reduced velocity $\bar{V}$.

The experimental results in Fig. 4 give $(|\dot{z}|/V)_{min} < 0.40$, i.e., they are bounded by Eq. (2). However, the margin is less than 30%, indicating that Eq. (2) provides a realistic, not unreasonably conservative, upper limit.

As $|\dot{z}|/V = 2\pi f \Delta z/V$, Eq. (2) gives

$$(\Delta z/h)_{lim} < 0.09\bar{V} \qquad (3)$$

In Fig. 11 this limit is compared with theoretical and experimental results for a square cross section. Part of the slope difference between prediction[6] and experiment[9,19] for $c/h = 1$ is caused by the presence of mechanical damping in the experiment, as was discussed in Ref. 6. If the test had been performed in water instead of in air the experimental results would have fallen closer to the prediction for $c/h = 1$. In

regard to the response of the quadratic cross section, $c/h=1$ in Fig. 11, the results from Ref. 19 show the response to start at $\bar{V}\approx 8.5$ due to the interaction with the Karman vortex shedding. This causes an initial fast increase of the amplitude response. However, it approaches the galloping limit from below in an asymptotic fashion.

As $\bar{V}=V/fh$, Eq. (3) can also be written

$$(\Delta z)_{\lim} < 0.09V/f \tag{4}$$

That is, the limit amplitude defined by Eq. (3) is insensitive to both the size and the shape of the cross section. For the somewhat typical values[18] $f=1$ Hz and $V=30$ mph Eq. (3) gives

$$(\Delta z)_{\lim} < 3.8\text{ft} \tag{5}$$

In the present analysis no torsional oscillations have been included. Although the torsional oscillation in itself may introduce critical structural loads,[3,4] it has no effect on the results expressed by Eqs. (2-4). Adding a torsional amplitude will simply decrease the value $|\dot{z}|/V$ needed to exceed α_2, and will therefore only decrease $(|\dot{z}|/V)_{\lim}$ and $\Delta z_{\lim}$ (this does not contradict the fact that for some cases of the icing cable the torsional motion may itself be needed to generate negative lift).

The limiting amplitude given by Eqs. (2-4) applies only for plunging oscillations, e.g., of a stiff beam. For a structurally deforming or deflecting cable, submarine mast, or other large-span structure, the galloping limit cycle amplitude can be computed using the presented two-dimensional results in the analysis. It should be noted, however, that in the analysis of a galloping cable, or a structural beam describing bending oscillations, it cannot be assumed that the sudden change of flow separation or reattachment conditions occurs simultaneously over the complete span, as the midspan location will exceed $\dot{z}/V=\alpha_2$ before the rest of the span. One might have expected that this change in flow condition would spread gradually from midspan toward the end supports, as the various spanwise stations reach the local value $\dot{z}/V=\alpha_2$. However, this is not what happens. Tarzanin[20] found that, on a helicopter blade, the stall did not start at the tip and spread gradually inward on the retreating blade as the stall angle was exceeded. Instead, stall started simultaneously over the outboard 40% of the blade span. Correspondingly, one would have to assume that reattachment occurs simultaneously over the 40% midspan portion of the three-dimensional galloping cable.

Conclusions

Theoretical and experimental results for galloping cables show that the final large amplitude response is of the self-excited type and is not affected by the Karman vortex shedding. An analysis is presented which defines the maximum possible galloping amplitude of an arbitrary cross section, thereby providing the designer with a simple, fast method to determine whether or not he has to take a closer look at the often very complicated problem of dynamic response to separated flow.

References

[1] Blevins, R. D., *Flow-Induced Vibration*, Van Nostrand Reinhold Co., New York, 1977, pp. 55-57.

[2] Parkinson, G. V., "Mathematical Models of Flow-Induced Vibration of Bluff Bodies," *Flow-Induced Structural Vibrations*, edited by E. Naudascher, Springer Verlag, Berlin, 1974, pp. 81-127.

[3] Ericsson, L. E. and Reding, J. P., "Aeroelastic Analysis of the Shuttle External Tank Cable Trays," Lockheed Missiles and Space Co., Sunnyvale, Calif., Final Tech. Rept. LMSC-D766543, Contract ASO-751485, April 1981.

[4] Ericsson, L. E. and Reding, J. P., "Aeroelastic Stability of Space Shuttle Proturberances," *Journal of Spacecraft and Rockets*, Vol. 19, July-Aug. 1982, pp. 307-313.

[5] Ericsson, L. E. and Reding, J. P., "Potential Hydroelastic Instability of Profiled Underwater Structures," *Journal of Hydronautics*, Vol. 14, Oct. 1980, pp. 97-104.

[6] Ericsson, L. E., "Hydroelastic Effects of Separated Flow," *AIAA Journal*, Vol. 21, March 1983, pp. 452-458.

[7] Ericsson, L. E., "Karman Vortex Shedding and the Effect of Body Motion," *AIAA Journal*, Vol. 18, Aug. 1980, pp. 935-944, Errata: *AIAA Journal*, Vol. 21, March 1983, p. 480.

[8] Polhamus, E. C., "Effect of Flow Incidence and Reynolds Number on Low-Speed Aerodynamic Characteristics of Several Non-Circular Cylinders with Applications to Directional Stability and Spinning," NASA TR R-29, 1959.

[9] Laneville, A. and Parkinson, G. N., "Effect of Turbulence on Galloping of Bluff Cylinders," *Proceedings of Conference on Wind Effects on Buildings and Structures*, 1971, pp. 787-797.

[10] Klebanoff, P. S., "Characteristics of Turbulence in a Boundary Layer with Zero Pressure Gradient," NACA-R-1247, 1955.

[11] Parkinson, G. V., "Aeroelastic Galloping in One Degree of Freedom," *Proceedings of the Conference on Wind Effects on Buildings and Structures*, held at NPL, England, June 1963, Vol. II, Her Majesty's Stationary Office, London, 1965, pp. 582-609.

[12] Nakamura, Y. and Mizota, T., "Aerodynamic Characteristics and Flow Patterns of a Rectangular Block," *Reports of Research Institute for Applied Mechanics*, Kyushu Univ., Japan, Vol. XIX, No. 65, March 1972, pp. 289-294.

[13] Ericsson, L. E., "Unsteady Aerodynamics of Separating and Reattaching Flow on Bodies of Revolution," *Recent Research on Unsteady Boundary Layers*, Vol. 1, IUTAM Symposium, Laval Univ., Quebec, May 24-28, 1971, pp. 481-512.

[14] Ericsson, L. E. and Reding, J. P., "Review of Vortex-Induced Asymmetric Loads—Part I," *Z. Flugwiss*, Weltraumforsch, 5, Heft 3, 1981, pp. 162-174.

[15] Ericsson, L. E. and Reding, J. P., "Review of Vortex-Induced Asymmetric Loads—Part II," *Z. Flugwiss*, Weltraumforsch., 5, Heft 6, 1981, pp. 349-366.

[16] Reding, J. P. and Ericsson, L. E., "Maximum Side Forces and Associated Yawing Moments on Slender Bodies," *Journal of Spacecraft and Rockets*, Vol. 17, Nov.-Dec. 1980, pp. 515-521.

[17] Hogg, A. D. and Edwards, A. T., "The Status of the Conductor Galloping Problem in Canada," *Proceedings of the Conference on Wind Effects on Buildings and Structures*, held at NPL, Her Majesty's Stationary Office, London, England, 1965, pp. 562-580.

[18] Ericsson, L. E. and Reding, J. P., "Unsteady Airfoil Stall," NASA CR-66787, July 1969.

[19] Nakamura, Y. and Mizota, T., "Unsteady Lifts and Wakes of Oscillating Rectangular Prisms," *Journal of Engineering Mechanics Div., Proceedings of the American Society of Civil Engineers*, Vol. 101, No. EM6, Dec. 1975, pp. 858-871.

[20] Tarzanin, F. J. Jr., "Prediction of Control Loads Due to Blade Stall," *Journal of the American Helicopter Society*, Vol. 17, April 1972, pp. 33-46.